Erciyes University Journal of Institue Of Science and Technology

Research Article
10.65520/erciyesfen.1927039

Imprint:
Volume: 42(2)
Year: 2026
Page: 701-720

Seismic Performance Assessment of a Reinforced Concrete School Building

Sercan Şahin[a]
R. Tuğrul Erdem[b*]
Tolga Yılmaz[c]
Mehmet Kamanlı[d]

[a] Master's Student, Manisa Celal Bayar University, sercansahinonline@gmail.com
[b] Prof., Manisa Celal Bayar University, tugrul.erdem@cbu.edu.tr
[c] Assoc. Prof., Konya Technical University, tyilmaz@ktun.edu.tr
[d] Prof., Konya Technical University, mkamanli@ktun.edu.tr

* Corresponding Author

Received: 4/10/2026
Accepted: 6/30/2026

Citation:
Sercan Şahin, R. Tuğrul Erdem, Tolga Yılmaz, Mehmet Kamanlı (2026). Seismic Performance Assessment of a Reinforced Concrete School Building. *Erciyes University Journal of Institue Of Science and Technology*, 42(2), 701-720. https://doi.org/10.65520/erciyesfen.1927039

Abstract

Earthquakes represent one of the major natural hazards affecting structural safety in Türkiye due to the country's location along active fault systems. Recent destructive earthquakes have highlighted the necessity of reassessing the seismic performance of the existing reinforced concrete (RC) building stock, particularly structures constructed according to older design codes. According to the Turkish Building Earthquake Code 2018 (TBEC 2018), school buildings are classified as public facilities that are expected to remain operational after earthquakes; therefore, they must provide sufficient structural performance to ensure life safety and continuity of service. In this study, the seismic performance of an existing RC school building was evaluated by ProtaStructure 2026 structural analysis software. Building survey studies, including concrete cover removal, reinforcement scanning, and tests conducted to determine the concrete compressive strength, were carried out through detailed on-site investigations. Based on the obtained data, a three-dimensional structural model was developed, and seismic hazard parameters, local soil conditions, and material properties corresponding to the building location were incorporated into the structural model. Subsequently, nonlinear incremental pushover analyses were performed for the DD-1 and DD-3 earthquake ground motion levels defined in TBEC 2018. The analysis results indicated that some structural members reached the advanced damage and collapse regions, demonstrating that the building does not satisfy the target performance levels specified in the code. The findings reveal that detailed seismic performance assessment of existing reinforced concrete public buildings using advanced analytical methods is of critical importance for accurately evaluating structural safety.

Keywords: ProtaStructure, Reinforced concrete, School building, Nonlinear analysis, Seismic performance

Betonarme Bir Okul Binasının Deprem Performansının Değerlendirilmesi

Öz

Depremler, Türkiye'nin aktif fay sistemleri üzerinde yer alması nedeniyle yapısal güvenliği etkileyen başlıca doğal afetlerden biridir. Son yıllarda meydana gelen yıkıcı depremler, özellikle eski tasarım yönetmeliklerine göre inşa edilmiş mevcut betonarme yapı stokunun deprem performansının yeniden değerlendirilmesi gerekliliğini ortaya koymuştur. Türkiye Bina Deprem Yönetmeliği 2018'e (TBDY-2018) göre okul binaları, deprem sonrasında hizmet vermeye devam etmesi beklenen kamu yapıları arasında sınıflandırılmaktadır. Bu nedenle, hizmet sürekliliğinin sağlanabilmesi için yeterli performansı sağlamaları gerekmektedir. Bu çalışmada, mevcut betonarme bir okul binasının deprem performansı ProtaStructure 2026 yapısal analiz programı kullanılarak değerlendirilmiştir. Yapıya ait rölöve çalışmaları, beton örtüsünün kaldırılması, donatı taraması ve beton basınç dayanımını belirlemek amacıyla gerçekleştirilen çalışmalar ayrıntılı yerinde incelemeler yoluyla belirlenmiştir. Elde edilen veriler doğrultusunda, yapının üç boyutlu yapısal modeli oluşturulmuş ve yapının bulunduğu konuma ait deprem tehlike parametreleri, yerel zemin koşulları ve malzeme özellikleri yapısal modele tanımlanmıştır. Daha sonra TBDY-2018'de tanımlanan DD-1 ve DD-3 deprem yer hareketi düzeyleri için doğrusal olmayan artımsal itme analizleri gerçekleştirilmiştir. Analiz sonuçları, bazı taşıyıcı elemanların ileri hasar ve göçme bölgelerine ulaştığını ve yapının yönetmelikte tanımlanan hedef performans düzeylerini sağlamadığını göstermiştir. Bu bulgular, mevcut betonarme kamu yapılarının deprem performanslarının ayrıntılı analiz yöntemleri ile değerlendirilmesinin yapısal güvenliğin belirlenmesi açısından kritik önem taşıdığını ortaya koymaktadır.

Anahtar kelimeler: ProtaStructure, Betonarme, Okul binası, Doğrusal olmayan analiz, Deprem performansı

1. INTRODUCTION

Türkiye is located in a seismically active region due to its geological position along major active fault systems. Situated on the Alpine–Himalayan seismic belt, the country frequently experiences earthquakes of varying magnitudes generated by the North Anatolian, East Anatolian, and Western Anatolian fault systems [1,2]. Historical and recent earthquake records indicate that these events have caused significant loss of life and property [13,14]. These observations highlight that the existing building stock contains various deficiencies in terms of seismic safety. Consequently, evaluating the seismic performance of existing structures and identifying appropriate improvement measures have become important engineering challenges [7].

In recent years, destructive earthquakes have emphasized the necessity of systematically assessing the seismic performance of existing reinforced concrete (RC) buildings and identifying their structural deficiencies under current seismic code requirements. In this context, the Turkish Building Earthquake Code-2018 (TBEC-2018) defines in detail both the design principles for new buildings subjected to seismic actions and the analysis and evaluation procedures for assessing the seismic performance of existing buildings [3]. Within the framework of this code, spectral parameters corresponding to different earthquake ground motion levels are determined based on material properties, local soil conditions, and the seismic hazard data provided by the Turkish Earthquake Hazard Map. Furthermore, the seismic behavior of structures under these earthquake effects is evaluated using a performance-based assessment approach [4-7].

Public buildings that are expected to remain operational after an earthquake, particularly school buildings, represent critical facilities that must ensure not only life safety but also continuity of service following seismic events [8-10]. However, a significant portion of the existing public building stock in Türkiye was designed and constructed according to earlier seismic regulations that were based on lower seismic demands. As a result, reassessing the seismic performance of these structures under the requirements of current seismic codes has become necessary. Accordingly, the number of studies focusing on the seismic performance evaluation of existing public buildings has increased significantly in the literature [11-14].

Seismic performance can be defined as a measure of the expected structural behavior and damage level of a building under a specified earthquake ground motion level. Within the scope of TBEC-2018, this performance can be evaluated using either linear or nonlinear analysis methods. Nonlinear analysis methods are widely preferred for assessing existing structures because they are capable of representing plastic deformations, damage mechanisms, and potential collapse behavior of structural members in a more realistic manner [15-21]. In addition, with the advancement of computational capabilities and numerical solution techniques, nonlinear time-history analysis methods based on recorded earthquake acceleration time histories have also become increasingly common in the literature [22-24].

Studies conducted on the seismic performance of existing reinforced concrete buildings, together with post-earthquake damage observations, reveal that similar structural deficiencies tend to recur in different types of structures. These deficiencies mainly arise from insufficient material strength, design and detailing errors during the design stage, construction defects during the implementation process, and inadequate reinforcement detailing in beam–column joint regions. In addition, structural irregularities such as short-column effects, soft-story configurations, and stiffness irregularities significantly influence the seismic behavior of buildings. These structural weaknesses make it necessary to conduct detailed seismic performance assessments of existing reinforced concrete buildings and to support reliable engineering decisions regarding possible intervention needs [25,26].

In this study, the seismic performance of an existing reinforced concrete public school building was investigated using nonlinear incremental pushover analysis. The structure was modeled in three dimensions using ProtaStructure 2026 software, taking into account the existing soil conditions, material properties, and reinforcement details identified through field investigations and material testing [27]. Based on the analysis results, the damage states of structural members were evaluated and the ability of the building to satisfy the target performance levels defined in TBEC-2018 was assessed. Although numerous studies have investigated the seismic performance of reinforced concrete buildings, detailed case studies integrating comprehensive field investigations, material characterization, and code-based nonlinear performance assessment of existing public-school buildings remain relatively limited. Unlike many previous studies that focus primarily on analytical performance evaluation, this research combines detailed field investigations, nonlinear performance analysis, and code-based assessment of an existing public-school building designed according to earlier seismic practices. Therefore, the findings of this study are expected to provide practical insights for the seismic assessment of existing reinforced concrete public buildings with similar structural characteristics and highlight the influence of actual material properties and structural deficiencies on overall seismic performance.

2. MATERIALS AND METHODS

In this study, the investigated structure is an existing reinforced concrete (RC) school building serving public use. The building consists of three typical stories with a total footprint area of 513.71 m^2 and a uniform story height of 3.30 m. The structural system is composed of reinforced concrete moment-resisting frames, while the floor system consists of beam-supported slabs. General views of the structure are presented in Figure 1, whereas the building formwork plans are shown in Figures 2 and 3. Although the overall structural layout of the building is generally similar between the floors, there are differences in the arrangement of certain columns and shear walls between the typical floors and the third floor. Therefore, the formwork plans are presented separately. These graphical representations provide the basis for identifying the geometric characteristics of the building, as well as its structural system configuration and overall plan layout. The case study building is located in the Aegean Region of Türkiye.

Figure 1. Building elevations

Figure 2. Formwork plans of the first and second floors

Figure 3. Formwork plans of the third floor

Comprehensive field investigations were conducted on the existing building to determine the material and reinforcement properties of the structural system. Laboratory tests were carried out on core samples extracted from selected structural elements in order to evaluate the compressive strength of the concrete. The core samples were tested in an accredited laboratory in accordance with the relevant standards for core sampling and compression testing. The obtained compressive strength values were then used to define the concrete material properties in the numerical model. Based on the obtained test results, the existing concrete was classified as C14. These results provided the basis for defining the material properties used in the structural modeling and analysis of the building.

To determine the properties of the reinforcement steel used in the structural elements, the cover removal method was applied and a reinforcement scanning device was utilized to identify the reinforcement layout and bar diameters. The investigations indicated that the reinforcement steel used in the structural members corresponds to grade S420. These findings were subsequently used to characterize the strength and ductility behavior of the structural members in the analytical model.

During the field investigations, it was also observed that in some structural elements the stirrups were irregularly spaced, and in certain regions the spacing exceeded the limits prescribed by current design codes, resulting in limited confinement effectiveness. In addition, inadequate hook details and incomplete closed stirrup arrangements were identified, which do not fully comply with the ductility requirements specified in modern seismic design codes. Such deficiencies in reinforcement detailing are expected to adversely affect the ductility capacity and seismic performance of the structural members. The field procedures used for reinforcement detection and core sampling are illustrated in Figures 4 and 5.

Figure 4. Reinforcement detection and cover removal procedures

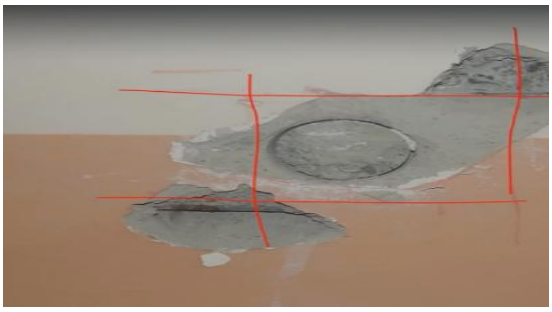

Figure 5. Concrete core sampling procedure

The field investigations were carried out in accordance with the data collection procedures for the assessment of existing buildings specified in Articles 15.2.4.2 and 15.2.4.3 of the 2018 Turkish Building Earthquake Code (TBEC-2018). Within this framework, the concrete cover was removed in at least 5% of the columns and shear wall elements on each floor to directly identify the longitudinal and transverse reinforcement layout. In addition, the reinforcement details of at least one beam per floor were determined through concrete cover removal. For the columns and shear walls where cover removal was not performed, a reinforcement scanning device was employed in at least 20% of the elements to identify the reinforcement arrangement, bar diameters, and spacing. To determine the compressive strength of the concrete, core samples were extracted from at least three columns and shear walls on each floor in accordance with TBEC-2018 provisions, and laboratory tests were conducted on these samples [1].

A comparison between the minimum number of inspections and samples required by TBEC-2018 and those performed in this study for concrete cover removal, reinforcement scanning, and core sampling is presented in Table 1. In addition, the cross-sectional properties, bar diameters, and reinforcement layout details of the columns, shear walls, and beams identified during the field investigations are provided in Tables 2 and 3. These data form the basis for accurately characterizing the structural system of the existing building and for defining the material and reinforcement parameters used in the structural analysis model developed in accordance with TBEC-2018 provisions. In this context, the number of reinforcement scans was determined based on 20% of the columns and shear walls where concrete cover removal was not performed. Besides, cross-section details of the vertical structural members are presented between Figures 6 and 9.

Table 1. Experimental results of concrete samples

Floor	Number of columns and shear walls	Cover removal 5% of (C+SW)	Scanning 20% of C+SW	Number of beams	Beam cover removal	Scanning 10% of beams	Core samples
1	23	2	5	35	1	4	3
2	23	2	5	35	1	4	3
3	23	2	5	39	1	4	3
Total	69	6	15	109	3	12	9

Table 2. Column cross-sectional sizes and reinforcement details

Floor	Column number	Section sizes (cm)	Longitudinal reinforcement	Transverse reinforcement
1	S1, S2, S3, S4, S5, S6, S9, S10, S11, S12	40×60	14Ø14	Ø8/15
	S7, S8	70×35	14Ø14	Ø8/15
2	S1, S2, S3, S4, S5, S6, S9, S10, S11, S12	40×60	14Ø14	Ø8/15
	S7, S8	70×35	14Ø14	Ø8/15
3	S1, S2, S3, S4, S5, S6, S9, S10, S11, S12	40×60	14Ø14	Ø8/15
	S7, S8	70×35	14Ø14	Ø8/15

Table 3. Shear-wall cross-sectional sizes and reinforcement details

Floor	Shear-wall number	Section sizes (cm)	Top reinforcement	Web reinforcement	Transverse reinforcement
1	P1, P2, P3, P4	30 × 790	11Ø12 × 2	29Ø16 × 2	Ø8 / 15
	P5, P6, P8, P9, P10, P11	30 × 430	11Ø12 × 2	16Ø16 × 2	Ø8 / 15
	P7	30 × 295	9Ø12 × 2	9Ø16 × 2	Ø8 / 15
2	P1, P2, P3, P4	30 × 790	11Ø12 × 2	29Ø16 × 2	Ø8 / 15
	P5, P6, P8, P9, P10, P11	30 × 430	11Ø12 × 2	16Ø16 × 2	Ø8 / 15
	P7	30 × 295	9Ø12 × 2	9Ø16 × 2	Ø8 / 15
3	P1, P2, P3, P4	30 × 790	11Ø12 × 2	29Ø16 × 2	Ø8 / 15
	P5, P6, P8, P9, P10, P11	30 × 430	11Ø12 × 2	16Ø16 × 2	Ø8 / 15
	P7	30 × 295	9Ø12 × 2	9Ø16 × 2	Ø8 / 15

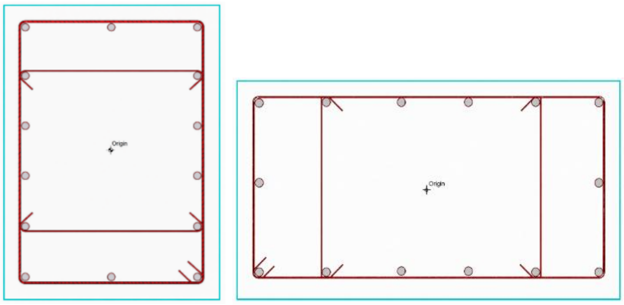

Figure 6. Column sections of 40x60 and 70x35 cm

Figure 7. Shear wall cross-section 30 × 790 cm

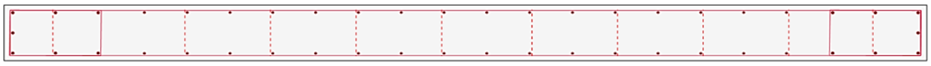

Figure 8. Shear wall cross-section 30 × 430 cm

Figure 9. Shear wall cross-section 30 × 295 cm

For illustrative purposes, the cross-sectional and reinforcement details of the beam elements located on the first floor are presented in Table 4. In addition, the reinforcement layout of beam K129, selected as a representative example of the existing beam reinforcement configuration, is shown in Figure 10.

Table 4. Reinforcement details of the beams

Beam number	Section sizes (cm)	Top Reinforcement	Top Additional Reinforcement	Bottom Reinforcement	Web Reinforcement	Transverse Reinforcement
K101	30×75	5Ø12	–	3Ø16	1Ø12	–
K102	30×75	5Ø12	–	3Ø16	1Ø12	Ø8/20/10
K105	30×75	5Ø12	3Ø14	4Ø18	1Ø12	Ø8/20/10
K106	30×75	5Ø12	2Ø12	3Ø16	1Ø12	Ø8/20/10
K108	30×75	5Ø12	2Ø12	3Ø16	1Ø12	Ø8/20/10
K109	30×75	5Ø12	2Ø16	4Ø18	1Ø12	Ø8/20/10
K110	30×75	5Ø12	–	3Ø16	1Ø12	Ø8/20/10
K111	30×75	5Ø12	–	3Ø16	1Ø12	Ø8/20/10
K115	30×75	5Ø12	–	3Ø16	1Ø12	Ø8/20/10
K116	30×75	5Ø12	6Ø14	3Ø16	1Ø12	Ø8/20/10
K117	30×75	5Ø12	2Ø12	3Ø16	1Ø12	Ø8/20/10
K118	30×75	5Ø12	–	3Ø16	1Ø12	Ø8/20/10
K119	30×75	5Ø12	2Ø12	3Ø16	1Ø12	Ø8/20/10
K120	30×75	5Ø12	4Ø16	3Ø16	1Ø12	Ø8/20/10
K125	30×75	5Ø12	–	3Ø16	1Ø12	Ø8/20/10
K126	30×75	5Ø12	–	3Ø16	1Ø12	Ø8/20/10
K127	30×75	5Ø12	–	4Ø18	1Ø12	Ø8/20/10
K128	30×75	5Ø12	2Ø14	3Ø16	1Ø12	Ø8/20/10
K129	30×75	5Ø12	2Ø12	3Ø16	1Ø12	Ø8/20/10
K130	30×75	5Ø12	2Ø12	3Ø16	1Ø12	Ø8/20/10
K132	30×75	5Ø12	–	3Ø16	1Ø12	Ø8/20/10
K133	30×75	5Ø12	–	3Ø16	1Ø12	Ø8/20/10
K134	30×75	5Ø12	–	3Ø16	1Ø12	Ø8/20/10

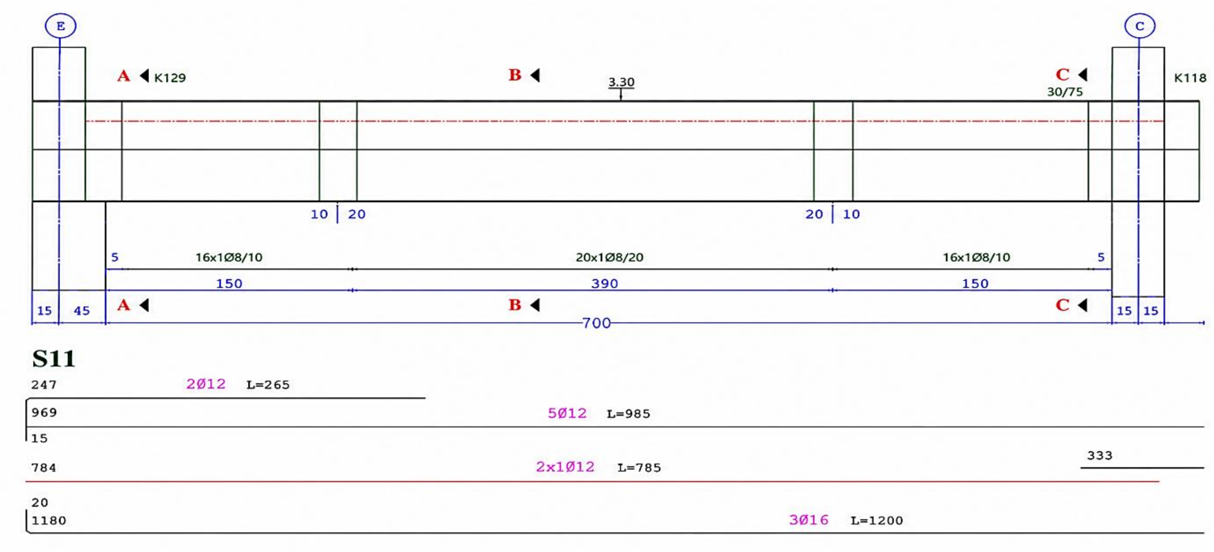

Figure 10. Reinforcement details of K129

In evaluating the site conditions, the soil was classified as ZB in accordance with TBEC-2018, considering the presence of slightly weathered to moderately strong rock formations. The slab thickness throughout all stories of the building is 15 cm, and the imposed live loads acting on the slabs were defined as 2.00 kN/m^2 for typical floors and 3.00 kN/m^2 for the roof, taking into account the additional roof loads [28]. The building walls were modeled as two types: 30 cm-thick insulated exterior walls and 15 cm-thick non-insulated interior walls, whose effects were incorporated into the structural model as dead loads.

The existing concrete strength, reinforcement properties, soil parameters, and seismic hazard data obtained from field investigations, material tests, and reinforcement identification studies were defined in the structural model representing the current condition of the building. Using the developed three-dimensional structural model, nonlinear performance analyses were performed for the DD-1 and DD-3 earthquake ground motion levels specified in TBEC-2018. Within this framework, the seismic response of the building was evaluated under the limited knowledge level approach, and the potential damage mechanisms of the structural members were examined to determine whether the building satisfies the target performance levels.

3. SEISMIC PERFORMANCE ANALYSIS

The seismic performance of the existing building was evaluated in accordance with the principles and procedures defined in Chapter 15 of the Turkish Building Earthquake Code (TBEC-2018). Within this framework, the building was modeled in a three-dimensional computational environment in order to reliably represent its behavior under seismic actions. The developed numerical model was defined to represent the existing structural characteristics of the building and served as the reference analytical model for the performance analyses conducted within the scope of TBEC-2018. The numerical model and performance assessments were developed using ProtaStructure 2026 software, which enables the implementation of code-based seismic performance evaluation procedures for existing buildings.

During the modeling stage, the data obtained from field investigations, material tests, and reinforcement identification studies presented in the previous sections were taken as the basis for the structural model. In order to represent the current condition of the building realistically, the columns, beams, and shear wall elements were modeled as frame elements in accordance with the assumptions defined in TBEC-2018. Story heights, structural grid layout, member continuity, and geometric properties were also incorporated into the numerical model. Through this approach, the stiffness characteristics of the structure under lateral loads, the load transfer mechanism between stories, and the overall behavior of the structural system were represented in the analysis model.

The developed three-dimensional structural model was defined in a manner that allows the identification of both plastic deformations at the member level and possible damage distributions within the entire structural system. Accordingly, the model was prepared to allow the application of nonlinear analysis procedures specified in TBEC-2018 and to evaluate the structural performance of the building under different earthquake ground motion levels. This approach enabled the reliable determination of the damage states of structural members, the formation of plastic hinges, and the overall structural performance levels. The frame element layout of the model and the three-dimensional numerical representation of the building are presented in Figure 11.

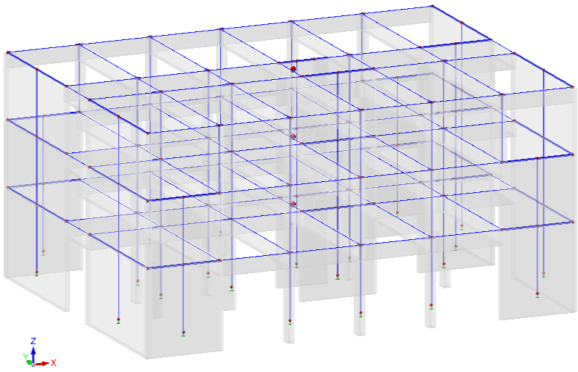

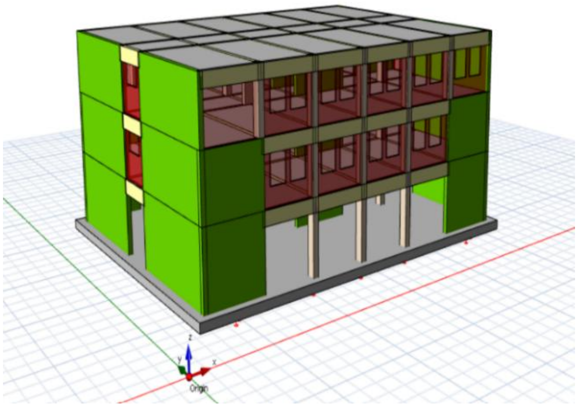

Figure 11. Structural model of the building

In accordance with the provisions of TBEC-2018, the analysis parameters required to define the seismic effects acting on the structure were determined after the structural model had been developed. Within this framework, the spectral acceleration coefficients corresponding to the elastic design spectrum were obtained by considering the seismic hazard parameters of the building location, the local soil class, and the earthquake ground motion levels defined in TBEC-2018. These parameters were subsequently assigned to the numerical model in order to accurately represent the seismic response of the structure under earthquake loading

For the performance evaluation, the earthquake ground motion levels DD-1 (maximum considered earthquake) and DD-3 (frequent earthquake), as defined in TBEC-2018, were taken into account. The spectral acceleration coefficients, characteristic period values, and other relevant seismic parameters corresponding to these earthquake levels were determined and incorporated into the analysis model. The spectral acceleration values and associated seismic parameters used for the DD-1 and DD-3 earthquake levels are presented in Table 5.

Table 5. Spectral parameters

Parameter	Value for DD-1	Value for DD-3
Short-period spectral acceleration coefficient, S_S	1.864	0.407
Spectral acceleration coefficient for 1.0 s period, S_1	0.522	0.101
Design spectral acceleration at short period, S_{DS}	1.678	0.366
Design spectral acceleration at 1.0 s period, S_{D1}	0.418	0.081

Within the scope of this study, the investigated building was classified as a structure that is required to remain operational after an earthquake. Accordingly, in accordance with the provisions of TBEC-2018, the building usage class was defined as BKS = 1, and the building importance factor was taken as I = 1.50. In evaluating the seismic performance of the structure, a deformation-based performance assessment approach was adopted, as it allows a more realistic representation of the behavior of the structural system. In this context, in accordance with the performance objectives defined in TBEC-2018, the target performance levels were specified as life safety (LS) for the DD-1 earthquake ground motion level and immediate occupancy (IO) for the DD-3 earthquake ground motion level.

Studies conducted in the field of earthquake engineering have shown that conventional force-based evaluation methods cannot adequately represent the nonlinear behavior of existing structures. In contrast, deformation-based nonlinear analysis methods provide more reliable results in determining structural performance. For this reason, nonlinear analysis procedures are widely used in the seismic performance evaluation of existing reinforced concrete buildings. In particular, nonlinear static analysis methods are frequently preferred in performance assessment studies because they enable the determination of structural capacity and damage distribution while maintaining relatively low computational cost and practical applicability in engineering practice. In the present study, nonlinear incremental pushover analysis was selected because it provides an effective and practical framework for evaluating the seismic performance and damage distribution of existing reinforced concrete buildings in accordance with TBEC-2018.

According to TBEC-2018, the damage states of reinforced concrete structural members under seismic actions are defined based on deformation limits at the critical sections of structural elements. These limits correspond to performance levels that are conceptually similar to the commonly used seismic performance limits of Immediate Occupancy (IO), Life Safety (LS), and Collapse Prevention (CP). The damage states defined in TBEC-2018 are determined according to the plastic deformations occurring at the critical regions of structural members. It should also be noted that this performance classification is not applicable to members exhibiting brittle behavior. The plastic deformation limits corresponding to these damage states and the associated damage regions for reinforced concrete members are defined in TBEC-2018, and a schematic representation of these damage regions is presented in Figure 12 [1].

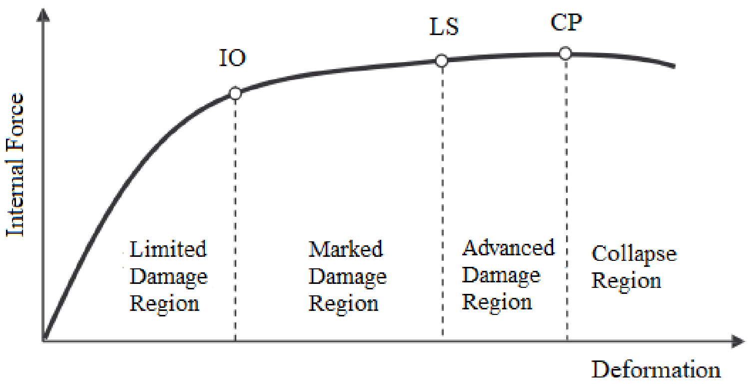

Figure 12. Damage limits

Nonlinear incremental pushover analysis, which is one of the nonlinear analysis methods, was performed to evaluate the nonlinear behavior of the structure under seismic effects. Within the scope of this method, the lateral loads acting on the structure were gradually increased according to a predefined load distribution pattern. During this process, the capacity curve representing the relationship between the base shear force and the roof displacement of the structure was obtained. Using this capacity curve, the plastic deformations occurring in the structural members, the sequence of damage formation, and the progression of damage within the structural system were evaluated as the displacement demand increased. Although nonlinear pushover analysis is widely used in engineering practice, it has certain limitations. Since the method is based on a predefined lateral load pattern, higher-mode effects and record-to-record variability associated with actual earthquake ground motions may not be fully represented. Nevertheless, the method provides a practical and reliable approach for the seismic performance assessment of existing reinforced concrete buildings and is widely accepted in current engineering practice and code-based evaluations.

4. ANALYSIS RESULTS

In accordance with the procedures defined in TBEC-2018, the capacity curve obtained from the pushover analysis was transformed into a modal capacity diagram through an appropriate coordinate transformation. The resulting modal capacity diagram was then evaluated together with the elastic design spectrum corresponding to the relevant earthquake ground motion level. Through this transformation, the structural response was expressed using an equivalent single-degree-of-freedom (SDOF) system approach, allowing the seismic performance of the structure to be assessed in spectral coordinates. This approach enables a direct comparison between the seismic demand imposed on the structure and its structural capacity.

The intersection point of the modal capacity diagram and the elastic design spectrum corresponding to the relevant earthquake ground motion level represents the performance point of the structure under that seismic demand. This performance point was used to determine the target displacement demand of the building and to evaluate the damage states of the structural members at that displacement level. The modal capacity diagrams obtained for the existing building, together with the corresponding seismic demand spectra, are presented in Figure 13 [1].

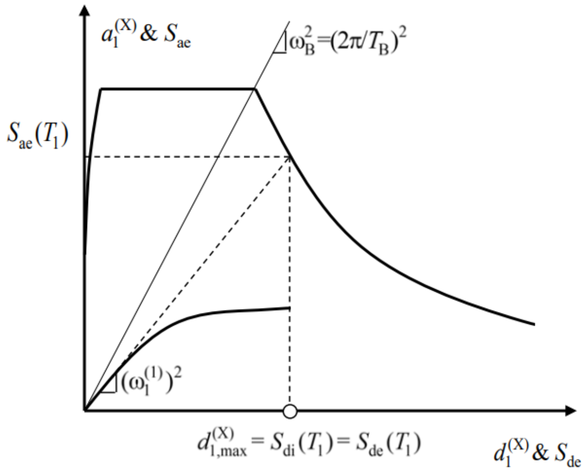

Figure 13. Modal capacity diagram and seismic demand spectrum

As a result of the nonlinear performance analyses conducted for the existing building, the target displacement values associated with the performance point were determined separately for each loading direction. Within this framework, the nonlinear behavior of the structure under seismic actions was evaluated, and the target displacement values corresponding to the intersection of the structural capacity and seismic demand were calculated. These displacement values served as the basis for determining the damage states of the structural members and assessing the overall performance level of the building.

For the DD-1 earthquake ground motion level, the target displacement values were obtained as 17.90 cm in the +x direction, 19.60 cm in the +y direction, 18.00 cm in the -x direction, and 19.70 cm in the -y direction. These results indicate that the structure experiences displacement demands of similar magnitude in different directions under seismic loading, while the structural response may vary depending on the loading direction.

For the DD-3 earthquake ground motion level, the target displacement values were determined as 3.70 cm in the +x direction, 3.50 cm in the +y direction, 3.50 cm in the -x direction, and 3.50 cm in the -y direction. Within the scope of the performance assessment, the structure was incrementally pushed up to the target displacement level determined for each earthquake ground motion level and loading direction. At these displacement levels, the plastic hinges formed in the structural members and the corresponding damage states were examined in detail. Based on the obtained damage distributions, performance evaluations were conducted at both the member and structural levels to determine whether the building satisfies the target performance levels defined in TBEC-2018.

For the specified loading directions, the performance evaluations were carried out based on the performance points obtained from the modal capacity diagrams. Within this framework, the calculation steps and numerical procedures used to determine the performance point for the +x and +y directions under the DD-1 earthquake ground motion level are presented in detail in Table 6. This table includes the calculation stages related to the transformation of the capacity curve into the modal capacity diagram, its comparison with the elastic design spectrum, and the determination of the performance point.

In addition, the modal capacity diagrams together with the corresponding elastic design spectra for the +x and +y directions under the DD-1 earthquake ground motion level are presented in Figures 14 and 15. These diagrams enable a graphical evaluation of the relationship between the seismic demand and the structural capacity of the building and serve as the basis for determining the target displacement values corresponding to the performance point. The fundamental periods of the structure were determined as T_{1x} = 0.177 s and T_{1y} = 0.117 s, corresponding to the first modes in the +x and +y directions, respectively.

Table 6. Target displacement calculation for DD-1 level

Parameter	Value at x direction	Value at y direction
The spectral displacement ratio determined based on the fundamental period values	$T_{x1} = 0.177, T_B = 0.249\ s \rightarrow C_R = 1.069$	$T_{y1} = 0.117, T_B = 0.249\ s \rightarrow C_R = 1.187$
Nonlinear spectral displacement associated with the fundamental period (T_1)	$S_{di(T_1)} = C_R \times S_{de(T_1)}$ $S_{di(T_1)} = 1.069 \times 0.136 = 0.145$ m	$S_{di(T_1)} = C_R \times S_{de(T_1)}$ $S_{di(T_1)} = 1.187 \times 0.153 = 0.181$ m
Modal single-degree-of-freedom (SDOF) system parameters	$\Gamma = 34.3747, \Phi_{di} = 0.03837$	$\Gamma = 36.4268, \Phi_{di} = 0.03516$
Target displacement	$U^P_{xN1} = \Phi_{di} \cdot \Gamma \cdot d^{(x)}_{1,max}$ $0.03837 \times 34.3747 \times 0.145 = 0.179$ m	$U^P_{yN1} = \Phi_{di} \cdot \Gamma \cdot d^{(y)}_{1,max}$ $0.03516 \times 36.4268 \times 0.181 = 0.196$ m

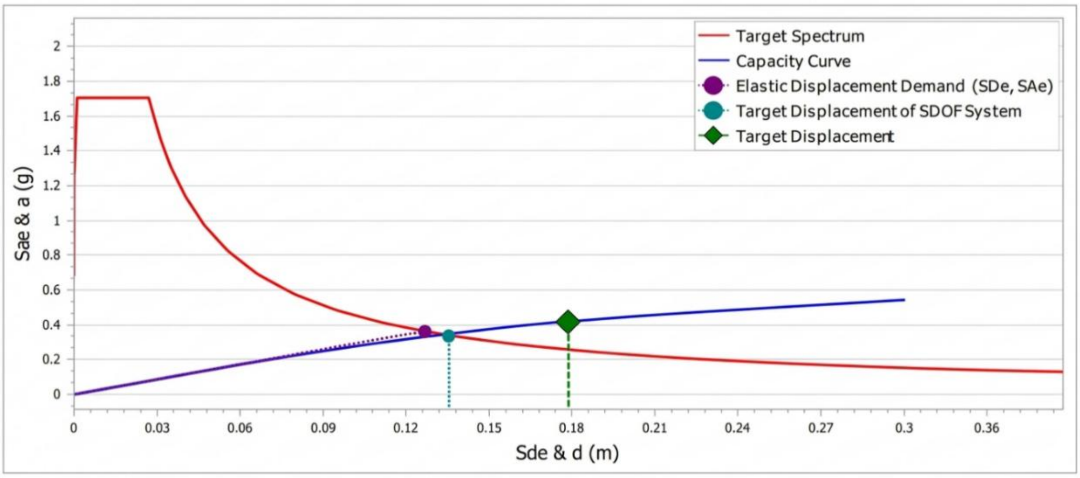

Figure 14. Capacity diagram and spectrum curve (+x, DD-1)

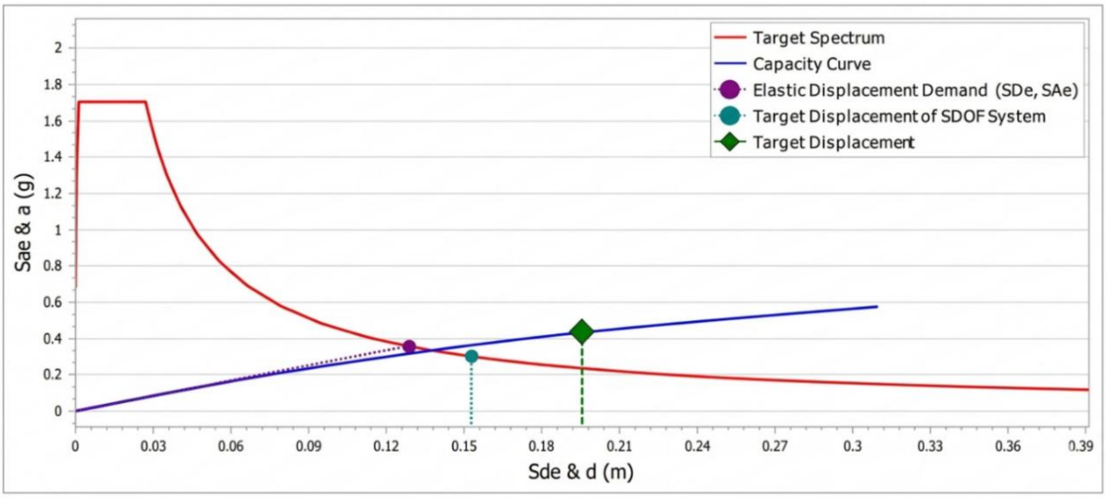

Figure 15. Capacity diagram and spectrum curve (+y, DD-1)

As a result of the nonlinear incremental pushover analyses performed for the considered earthquake ground motion levels, the damage regions occurring in the structural system members were evaluated in detail. Based on the analysis results obtained for the DD-1 and DD-3 earthquake ground motion levels, the damage states of columns, shear walls, and beams at each story level were determined considering the critical earthquake loading directions, and the corresponding damage distributions are presented in Tables 7 and 8. In these tables, the vertical load-bearing members, namely columns and shear walls, and the horizontal load-bearing members, namely beams, are classified separately, and the damage states of each element group are systematically presented.

Table 7. Damage regions for DD1 level

Element	Floor	LDR	MDR	ADR	CR	LDR	MDR	ADR	CR
		(+x direction)				(+y direction)			
Vertical	1. Floor	11	2	9	1	12	4	7	0
	2. Floor	13	10	0	0	13	10	0	0
	3. Floor	9	14	0	0	11	12	0	0
Beam	1. Floor	6	12	0	0	6	12	0	0
	2. Floor	8	10	0	0	9	9	0	0
	3. Floor	12	10	0	0	9	13	0	0

Table 8. Damage regions for DD3 level

Element	Floor	LDR	MDR	ADR	CR	LDR	MDR	ADR	CR
		(+x direction)				(+y direction)			
Vertical	1. Floor	23	0	0	0	23	0	0	0
	2. Floor	23	0	0	0	23	0	0	0
	3. Floor	23	0	0	0	23	0	0	0
Beam	1. Floor	6	12	0	0	6	12	0	0
	2. Floor	7	11	0	0	8	10	0	0
	3. Floor	17	5	0	0	17	5	0	0

To facilitate a clearer evaluation of the damage states occurring in the structural members for the DD-1 and DD-3 earthquake ground motion levels, the percentage distribution of elements within different damage regions was calculated based on the critical loading directions and presented graphically. Accordingly, diagrams illustrating the proportional distribution of structural members at different damage levels are provided in Figures 16 and 17. These graphs enable the evaluation of the damage distribution both at the member level and for the overall structural system under seismic actions.

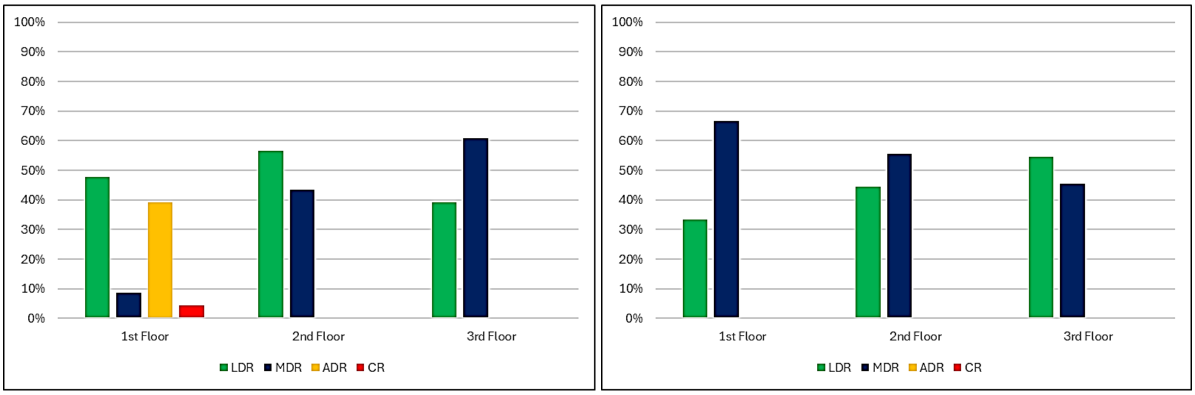

a) Vertical elements b) Beams

Figure 16. Damage distributions of structural elements for DD-1 earthquake level

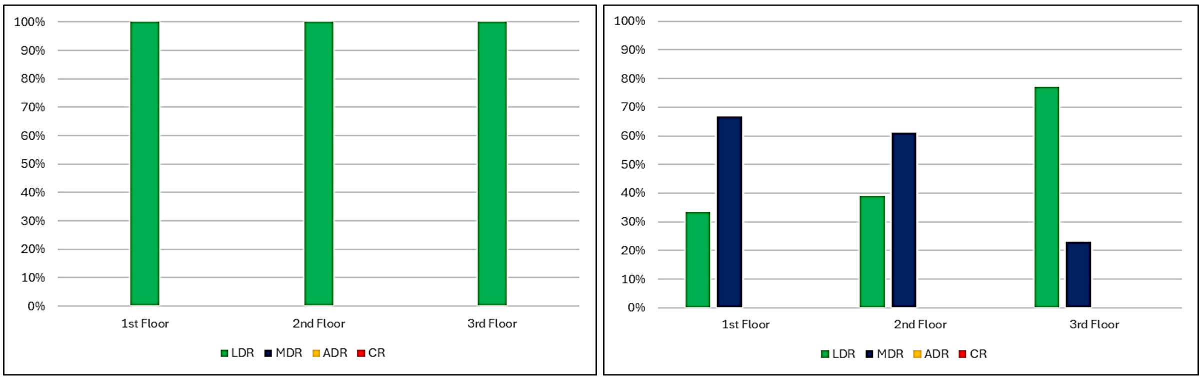

a) Vertical elements b) Beams

Figure 17. Damage distributions of structural elements for DD-3 earthquake level

Based on the field investigations, material tests, and nonlinear performance analyses conducted within the scope of this study, several structural deficiencies that adversely affect the seismic behavior of the existing reinforced concrete structure were identified. The low concrete strength determined through core tests reduced both the compressive capacity of the structural members and the bond between reinforcement and concrete, leading to earlier damage formation under seismic loading. In addition, although the reinforcement ratios of some beam members were found to be adequate, insufficient bond conditions prevented these elements from exhibiting the expected ductile behavior and resulted in the occurrence of significant damage. These observations indicate that the material properties and detailing characteristics of the existing structural members are limited in terms of satisfying the performance objectives defined in TBEC-2018.

Evaluations performed at the story level revealed that the stiffness and damage distribution were not homogeneous throughout the structure. In some stories, increased interstory drift demands were observed, leading to the occurrence of story irregularity effects. Although the L-shaped shear walls located at the corners of the plan contributed to the overall stiffness of the system, this stiffness contribution was not uniformly distributed among all structural members. In particular, beam members with relatively long spans were subjected to higher plastic rotation demands and consequently reached higher damage levels under seismic loading.

The performance analyses carried out for the DD-1 earthquake ground motion level showed that some column members reached the Severe Damage region, while a limited number of columns exhibited behavior corresponding to the Collapse region. These results indicate that the section capacity and ductility characteristics of the existing columns are insufficient to satisfy the Controlled Damage (CD) performance level targeted in TBEC-2018. These findings are consistent with previous studies reported in the literature, where low concrete strength, inadequate reinforcement detailing, and other structural deficiencies were identified as major factors leading to reduced seismic performance and increased damage in existing RC buildings [6-12]. The damage regions of the structural members of the existing building, determined based on the critical loading directions for the DD-1 and DD-3 earthquake levels, are presented in Figures 18 and 19.

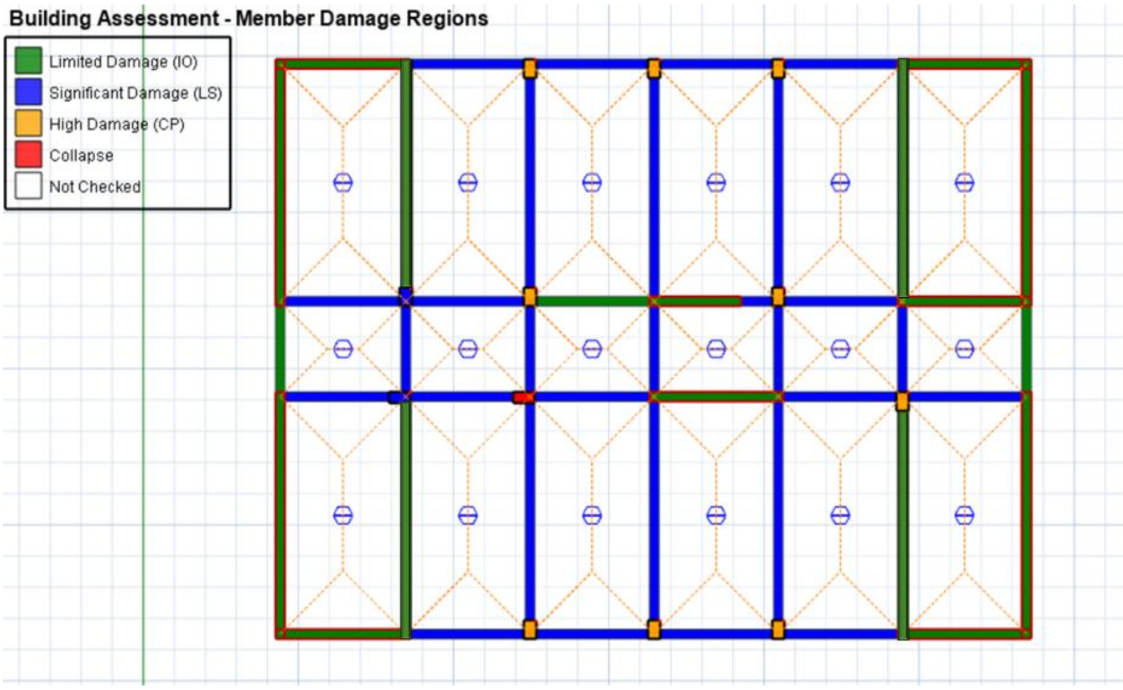

Figure 18. Damage regions of structural members for the DD-1 earthquake level

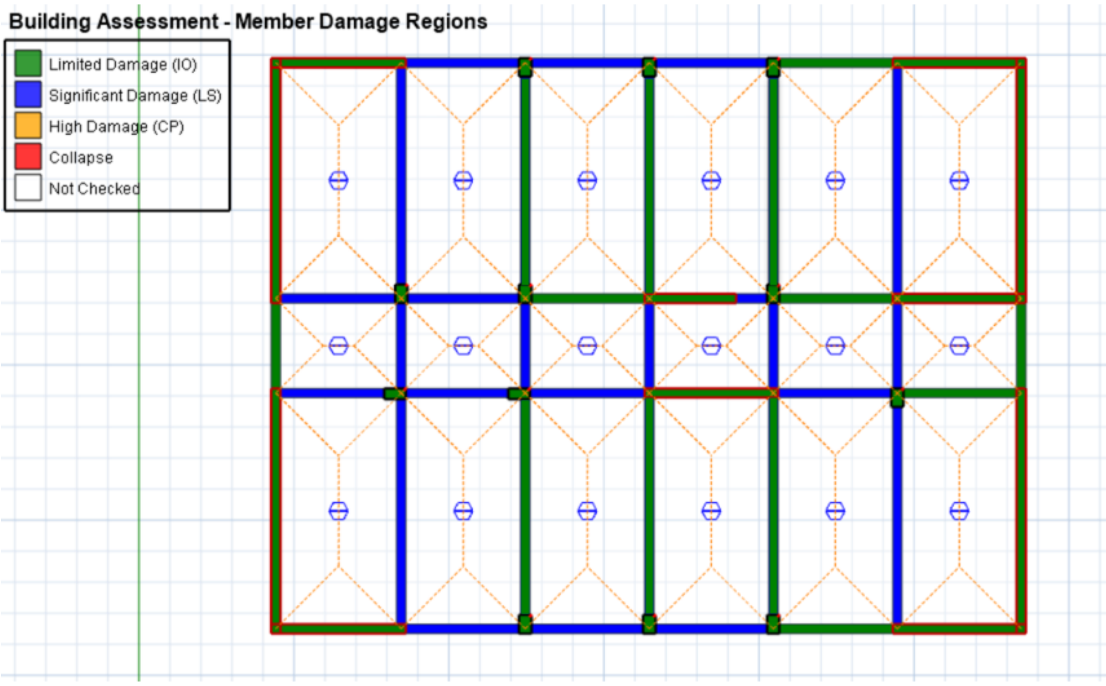

Figure 19. Damage regions of structural members for the DD-3 earthquake level

In addition, the three-dimensional (3D) plastic hinge damage distributions at the performance point obtained from the nonlinear incremental pushover analyses of the existing building under the DD-1 and DD-3 earthquake level, where more severe damage is expected, are presented in Figure 20.

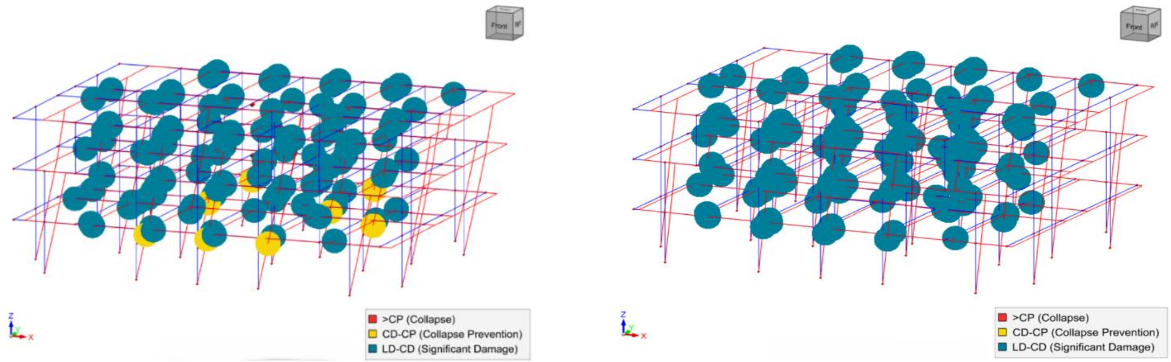

Figure 20. Plastic hinges for the DD-1 and DD-3 earthquake level

According to the Turkish Building Earthquake Code (TBEC-2018), the horizontal movement of vertical structural systems in the x or y direction under seismic effects is defined as displacement. The difference between the horizontal displacement of a vertical structural element at a given story and the displacement of the corresponding element at the story above or below is defined as the inter-story drift. The inter-story drift distributions obtained for each story of the existing building under the DD-1 and DD-3 earthquake ground motion levels in the critical loading direction are presented in Figure 21.

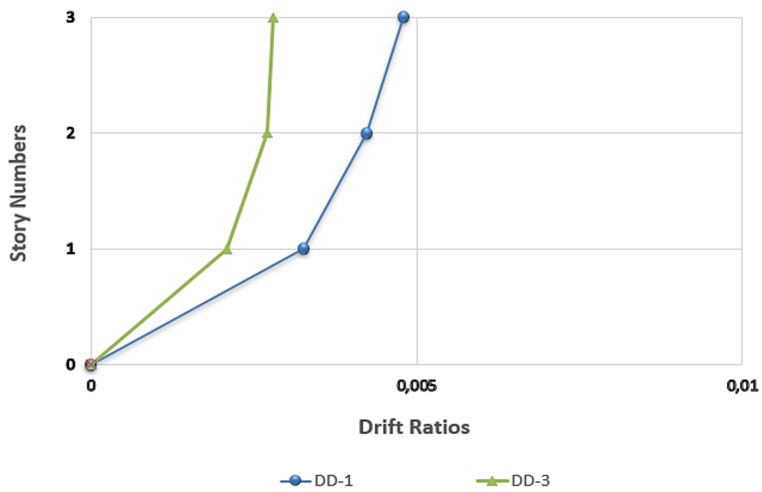

Figure 21. Inter-story drifts of the existing building for the DD-1 and DD-3 earthquake level

According to the provisions of TBEC-2018, the nonlinear analysis results of the building indicate that the inter-story drift values obtained under the DD-1 and DD-3 earthquake ground motion levels remain within the limits specified in the code. This demonstrates that the modeled structure satisfies the inter-story drift requirements defined by TBEC-2018. To visually illustrate the displacement distribution associated with the inter-story drift response of the building, the story-level displacements in the critical loading direction (+x) under the DD-1 earthquake level are presented in Figure 22.

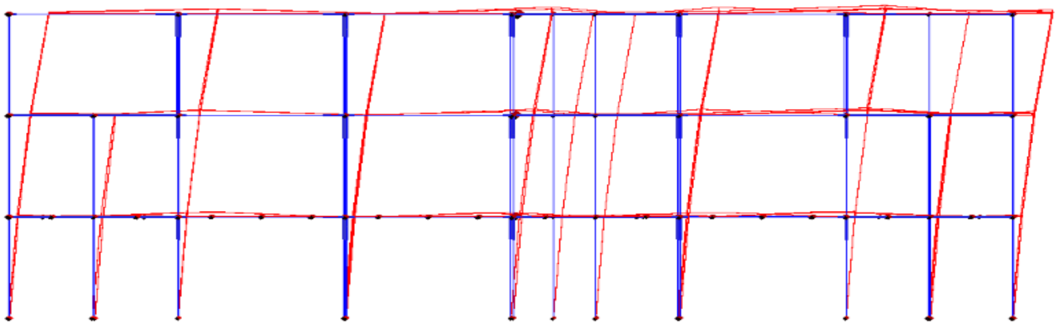

Figure 22. Story-level displacements of the building

4. CONCLUSION

Türkiye is located in a region characterized by significant seismic activity due to the presence of numerous active fault systems, and destructive earthquakes occur frequently throughout the country. Recent major earthquakes have clearly demonstrated the necessity of reassessing the seismic safety of the existing building stock. In this context, evaluating the seismic performance of reinforced concrete (RC) buildings, which constitute a large portion of the existing building stock, has become a critical requirement, particularly for public buildings that are expected to remain operational after an earthquake. When the target performance levels cannot be satisfied, further engineering decisions are required to determine the most appropriate intervention strategy for the structure.

Within the scope of this study, field investigations and material tests conducted on the investigated RC school building revealed several structural deficiencies that adversely affect the seismic performance of the load-bearing system. The most critical deficiencies were identified as low concrete compressive strength, limited bond performance between concrete and reinforcement, insufficient anchorage lengths, and irregular stirrup spacing. These deficiencies reduce the ductility capacity of structural members and contribute to the premature development of damage under seismic loading. Nonlinear pushover analyses were carried out to evaluate the seismic performance of the existing structure, and the corresponding target displacement values were calculated for each loading direction under the DD-1 and DD-3 earthquake ground motion levels. Based on the obtained performance points, the damage states of the vertical structural members (columns and shear walls) and beam elements were identified separately for each loading direction.

The damage states obtained from the nonlinear analyses were visually illustrated through the plastic hinge formations that developed at the end regions of the structural members. These plastic hinges provide a clear representation of the progression and concentration of damage within the structural system under increasing lateral displacement demands. In addition to the plastic hinge distributions, the inter-story drift ratios developed between adjacent stories were determined in order to evaluate the deformation compatibility and lateral displacement demands of the structure. Furthermore, the overall displacement patterns and deformation shapes of the building were presented graphically to illustrate the distribution of story-level displacements along the building height. These visual and quantitative evaluations allowed a comprehensive interpretation of the structural response and provided important insight into the deformation characteristics and damage propagation mechanisms of the building under seismic loading conditions.

The analysis results indicated that, under the DD-1 earthquake level, several vertical structural members reached the advanced damage region and a limited number of columns entered the collapse region, highlighting the insufficient strength and ductility capacity of the existing structural system. In addition, beam elements exhibited damage primarily within the significant damage region under both DD-1 and DD-3 earthquake levels, indicating that flexural demand was concentrated in these members as lateral displacement demands increased. These findings reveal that the structural deficiencies identified during the field investigations, such as low concrete strength and inadequate reinforcement detailing, significantly affected the nonlinear response of the building. Consequently, the existing structure was found to be unable to satisfy the target performance levels defined in TBEC-2018, namely the life safety performance level for the DD-1 earthquake ground motion level and the immediate occupancy performance level for the DD-3 earthquake ground motion level.

In conclusion, the detailed evaluation of existing reinforced concrete (RC) public buildings within the framework of TBEC-2018 through comprehensive performance analyses is of great importance for accurately identifying structural deficiencies and determining the seismic safety level of existing structures. The results obtained in this study demonstrate that field investigation data, material properties, reinforcement details, and nonlinear analysis results should be evaluated together in order to obtain a reliable assessment of existing public buildings. Therefore, the integrated evaluation of structural characteristics, material deficiencies, and code-based performance demands represents a critical component in the development of resilient and sustainable building policies. It is considered that the findings obtained from this study will contribute to the literature on the seismic performance assessment of existing RC public buildings and will provide useful guidance for future research and engineering applications in the field of earthquake engineering.

Peer-review: External, Independent.

Acknowledgements:
The authors would like to thank ProtaStructure for providing an academic license.

Declarations:

1. Statement of Originality:
This work is original.

2. Author Contributions:
Concept: SŞ,RTE; ***Conceptualization:*** SŞ,RTE; ***Literature Search:*** SŞ,TY,MK; ***Data Collection:*** SŞ; ***Data Processing:*** SŞ,TY,MK; ***Analysis:*** SŞ; ***Writing – original draft:*** RTE; ***Writing – review & editing:*** TY,MK.

3. Ethics approval:
Not applicable.

4. Funding/Support:
This work has not received any funding or support.

5. Competing Interests:
The authors declare no competing interests.

6. GenAI Usage Statement:
AI tools (ChatGPT) were used only for language editing and improvement.

7. Sustainable Development Goals:

REFERENCES

[1] Doğangün, A., Yön, B., Onat, O., Emin Öncü, M., Sağıroğlu, S. (2021). Seismicity of East Anatolian of Turkey and failures of infill walls induced by major earthquakes. Journal of Earthquake and Tsunami, 15(04), 2150017.

[2] Utkucu, M., Kurnaz, T. F., İnce, Y. (2023). The seismicity assessment and probabilistic seismic hazard analysis of the plateau containing large dams around the East Anatolian Fault Zone, Eastern Türkiye. Environmental Earth Sciences, 82(15), 371.

[3] TBEC-2018. (2018). Specifications for design of buildings under seismic effects. Ankara, Turkey.

[4] Gupta, P., Gupta, C. (2024). Seismic performance evaluation of reinforced concrete flat slab buildings using ETABS. Asian Journal of Civil Engineering, 25(7), 4995-5007.

[5] Ozkul, T. A., Kurtbeyoglu, A., Borekci, M., Zengin, B., Kocak, A. (2019). Effect of shear wall on seismic performance of RC frame buildings. Engineering Failure Analysis, 100, 60-75.

[6] Erdem, R. T. (2016). Performance evaluation of reinforced concrete buildings with softer ground floors. Gradevinar, 68(1), 39-49.

[7] Bento, S., Simoes, A. (2021). Seismic performance assessment of buildings. Buildings, 11(10), 440.

[8] Panahi, M., Rezaie, F., Meshkani, S. A. (2014). Seismic vulnerability assessment of school buildings in Tehran city based on AHP and GIS. Natural Hazards and Earth System Sciences, 14(4), 969-979.

[9] Zhang, J., Lata, A., Guo, X., Xu, Z. (2025). Seismic vulnerability assessment of reinforced concrete school buildings based on the concept of balanced seismic shear force distribution. Structures, 71, 108184.

[10] Ghimire, N., Chaulagain, H. (2021). Seismic vulnerability assessment of reinforced concrete school building in Nepal. Asian Journal of Civil Engineering, 22(2), 249-262.

[11] Kuria, K. K., Kegyes-Brassai, O. K. (2023). Nonlinear static analysis for seismic evaluation of existing RC hospital building. Applied Sciences, 13, 11626.

[12] Bilgin, H. (2015). Seismic performance evaluation of an existing school building in Turkey. Challenge Journal of Structural Mechanics, 1(4), 161-167.

[13] Ferreira, T. M., Rodrigues, H., Vicente, R. (2020). Seismic vulnerability assessment of existing reinforced concrete buildings in urban centers. Sustainability, 12(5), 1996.

[14] Gkournelos, P. D., Triantafillou, T. C., Bournas, D. A. (2021). Seismic upgrading of existing reinforced concrete buildings: A state-of-the-art review. Engineering Structures, 240, 112273.

[15] Erdem, R. T., Uyan, B. (2025). Evaluation of irregular reinforced concrete buildings according to different soil classes. Revista de la Construcción, 24(1), 183-195.

[16] Chopra, A. K., Goel, R. K. (2002). A modal pushover analysis procedure for estimating seismic demands for buildings. Earthquake Engineering and Structural Dynamics, 31(3), 561-582.

[17] Kalkan, E., Kunnath, S. K. (2007). Assessment of current nonlinear static procedures for seismic evaluation of buildings. Engineering Structures, 29(3), 305-316.

[18] Uva, G., Porco, F., Fiore, A. (2012). Appraisal of masonry infill walls effect in the seismic response of RC framed buildings: A case study. Engineering Structures, 34, 514-526.

[19] Ismaeil, M. (2018). Seismic capacity assessment of existing RC building by using pushover analysis. Civil Engineering Journal, 4(9), 2034-2043.

[20] Habibi, A., Izadpanah, M., Namdar, Y. (2022). A new modal lateral load pattern for improving pushover analysis to estimate nonlinear responses of structures. Australian Journal of Structural Engineering, 23(4), 289-302.

[21] Oz, I., Omur, M. (2025). Evaluating the seismic fragility and code compliance of turkish reinforced concrete buildings after the 6 February 2023 Kahramanmaraş earthquake. Applied Sciences, 15(10), 5554.

[22] Kwong, N. S., Chopra, A. K. (2018). Determining bidirectional ground motions for nonlinear response history analysis of buildings at far-field sites. Earthquake Spectra, 34(4), 1931-1954.

[23] Kalkan, E., & Chopra, A. K. (2010). Practical guidelines to select and scale earthquake records for nonlinear response history analysis of structures. U.S. Geological Survey Open-File Report 2010-1068.

[24] Vamvatsikos, D., Cornell, C. A. (2002). Incremental dynamic analysis. Earthquake Engineering and Structural Dynamics, 31(3), 491-514.

[25] Erdem, R. T., Karal, K. (2022). Performance evaluation and strengthening of reinforced concrete buildings. Revista de la Construcción, 21(1), 459-475.

[26] Latifi, R., Rouhi, R. (2020). Seismic assessment and retrofitting of existing RC structures: Seismostruct and seismobuild implementation. Civil Engineering and Architecture, 8(2), 84-93.

[27] ProtaStructure. (2026). ProtaStructure 2026. Prota Software, Ankara, Turkey.

[28] TS-498. (1997). Design loads for buildings. Ankara, Turkey.